A Full-Duplex Directional MAC Framework for Underwater Acoustic Sensor Networks

Qipei Liu, Gang Qiao, Suleman Mazhar, *Senior Member, IEEE*, Songzuo Liu, *Member, IEEE*, and Yi Lou, *Member, IEEE*

***Abstract*—Underwater acoustic communication plays an essential role in underwater wireless information exchange, and nodes with such an ability constitute an underwater acoustic sensor network (UASN). However, UASNs face many challenges, such as high bit error rate and high propagation delay, significantly reducing network performance. Because of the challenging nature of underwater environments, the power consumption and battery energy efficiency of sensor nodes need to be considered. Directional communication technology can conserve energy by restraining beam directivity and diminishing interference between nodes by enabling peer-to-peer communication with intended neighbors. However, the technology suffers from the problems of neighbor discovery, deafness effect, and hidden/exposed terminal. To address these challenges, we propose a full-duplex directional medium access control (MAC) framework based on the vector hydrophone and multimodal transducer in this paper, along with a benchmark MAC protocol, which enables adaptive power control to achieve spatial reuse and energy conservation. Simulation results show that the benchmark MAC protocol outperforms existing representative protocols in terms of throughput, end-to-end delay, and energy efficiency.**

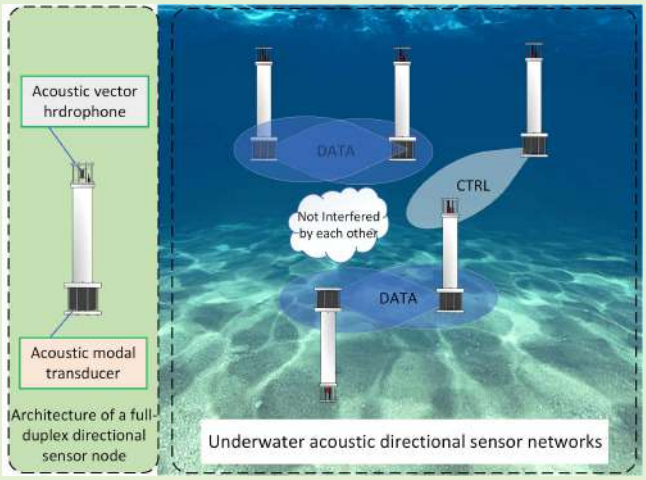

***Index Terms*—UASNs, full-duplex, directional communication, medium access control.**

I. Introduction

In RECENT decades, there has been significant interest in underwater acoustic sensor networks (UASNs) owing to their potential for application in the fields of marine exploration, early disaster warning, and coastal defense [1], [2]. The performance and robustness of UASNs have improved significantly during this period; however, many challenges remain unaddressed.

In particular, limited bandwidth, time-varying multipath, and low propagation speed [3] result in a high bit error rate and high latency, posing challenges for reliable communication and upper-layer protocol design. Consequently, the data rate for underwater communication is limited. A long time is required to transmit and receive a packet, incurring a high probability of collision and consequent retransmissions that drain the already constrained energy of the UASNs.

UASNs are characterized by the following main challenges [4], [5]:

- Low data rate (due to the low bandwidth of the underwater acoustic channel and the low speed of the acoustic signal).
- High delay, including propagation delay and transmission delay.
- High bit error rate.
- Minimal energy supply.
- The significant difference between the power required to receive or transmit an acoustic signal.

The power consumption for different operations varies in underwater communication. Typical transmission power is approximately a few tens of watts, and the power consumed for reception is 60 mW–2 W, and the standby consumption is approximately 1 mW [6]–[8]. As transmission is a costly behavior in UASNs, it is necessary to adopt measures to reduce energy waste, primarily due to packet collision-induced

Manuscript received 1 March 2022; revised 8 April 2022; accepted 20 April 2022. Date of publication 22 April 2022; date of current version 14 July 2022. This work was supported in part by the National Natural Science Foundation of China under Grant U1806201 and in part by the Natural Science Foundation of Heilongjiang Province of China under Grant LH2021F010. The associate editor coordinating the review of this article and approving it for publication was Prof. Jaime Lloret. *(Corresponding author: Yi Lou.)*

The authors are with the Acoustic Science and Technology Laboratory, Harbin Engineering University, Harbin 150001, China, also with the Key Laboratory of Marine Information Acquisition and Security (Harbin Engineering University), Ministry of Industry and Information Technology, Harbin 150001, China, and also with the College of Underwater Acoustic Engineering, Harbin Engineering University, Harbin 150001, China (e-mail: liuqipei@hrbeu.edu.cn; qiaogang@hrbeu.edu.cn; suleman@hrbeu.edu.cn; liusongzuo@hotmail.com; louyi@hrbeu.edu.cn).

Digital Object Identifier 10.1109/JSEN.2022.3169816

retransmissions. Some studies [9]–[12] proposed handshaking and reservation-based protocols to prevent collisions. However, owing to the problem of the hidden terminal (when a node cannot sense other nodes that may interfere with its transmission) and exposed terminal (when a node overhears another transmission that would not collide with it), retransmissions cannot be eliminated.

Some other studies have considered the solutions based on interference suppression for this problem, e.g., directional communication technology [13] to reduce energy dissipation and inter-node interference. In this way, a node can communicate with its intended receiver at a lower power without disturbing others, and the network lifetime is prolonged. Moreover, spatial reuse of a network is achieved, and throughput is improved. However, there are challenges to employing directional communication in UASNs. The neighbor discovery (ND) problem may be fundamental and crucial. Compared to traditional sensor networks that transmit and receive data omnidirectionally, the ND process becomes more complex and challenging for directional sensor networks [14] because the two nodes cannot communicate unless their antennas orient toward each other.

The deafness effect is an induced problem of directional technology that occurs when two nodes establish communication. However, their neighbors fail to overhear the ongoing packet exchange between the two communicating nodes [15]. If the neighbor attempts to initiate communication with the nodes at this time, it will not receive a response. Thus a back-off process will be launched, and this might lead to continuous back-off until the link status is misleadingly considered a failure [14].

In this paper, we focus on the above mentioned problems of underwater acoustic directional sensor networks (UADSNs) and propose a medium access control (MAC) framework based on the technologies of full-duplex communication [16] and directional communication. The framework exploits the collaboration of the vector hydrophone and the multimodal transducer. Furthermore, a MAC protocol based on the proposed framework is developed as a benchmark. The main contributions of this study are as follows:

1) The joint operational capability of the vector hydrophone and the multimodal transducer for UASNs is confirmed by analyzing their characteristics.
2) An energy consumption model is derived for directional transducers based on the acoustic intensity theory.
3) A full-duplex directional (FDD) MAC framework for UASNs is proposed to deal with the challenges introduced by the directional communication technology shown above, which combines the advantages of a full-duplex architecture.
4) Based on the proposed framework, a heuristic ND approach with time complexity $O(1)$ is presented for sparse UADSNs, which overcomes the drawbacks of the existing methods described in Section II.
5) A benchmark MAC protocol is elaborated, which exploits the spatial reuse of the channel and addresses the drawbacks that the related works in Section II presented, outperforming the existing classical approaches in UASNs by a large margin.

The rest of this paper is organized as follows. In Section II, some related works are discussed. In Section III, the system model is described, including the theoretical models of the vector hydrophone and multimodal transducer, as well as an energy consumption model. The proposed MAC framework is explained in Section IV, including the necessary services required for UADSNs, and in Section V, the FDD-MAC is elaborated. Simulation comparisons and evaluations are presented in Section VI. Finally, we conclude the paper in Section VII.

II. Related Works

Notably, most packet losses occur owing to data conflicts [17], [18], including transmission/reception conflict and reception/reception conflict [9], which results in acute retransmission and waste of already limited energy, thus reducing the network lifetime.

To address this problem, the authors in [11] proposed a dialog-based slotted floor acquisition multiple access (S-FAMA) protocol. It reduces very long control packet lengths and uses time slotting to avoid packet collisions without placing requirements on the size of the control packet, thereby conserving energy. However, the protocol requires nodes to be time-synchronized [19], which requires a complex synchronization algorithm or hardware.

In [12], the T-Lohi protocol introduced implicit contention to access a channel. A node that implements T-Lohi sends a short tone to contend for the channel and then listens to the channel for a certain period. If no other tones are heard in this period, the node accesses the channel; otherwise, it should back off according to the number of tones it receives and re-compete the channel until it becomes the only candidate. The protocol performs better in sparse and low-load networks; however, the hidden terminal and exposed terminal problems remain unaddressed. These contention-based MAC protocols avoid data collisions, but the long round-trip time (RTT) decreases channel utilization.

Reference [20] proposed an RC-MAC protocol that segregates the available bandwidth into a control channel with narrow bandwidth and a data channel with majority bandwidth. Reservations for the main channel are made by transmitting request-to-send (RTS) packets on the control channel. Thus, access to the channel is scheduled, and channel utilization is improved; however, the problem of exposed terminals remains.

Similarly, [21] proposed an idea to solve hidden/exposed terminal problems using full-duplex technology and presented a corresponding full-duplex distance-aware (FDDA) MAC protocol. Compared with the RC-MAC protocol, the channel and the roles to transmit and receive were duplicated. In this protocol, a modem has two sub-transducers that can transmit and receive asynchronously. When a potential exposed terminal emerges, the affected communicating node sends a delay-to-send (DTS) packet to reply to its RTS using the different transducer specialized for the control channel, preventing subsequent interruptions.

To improve the efficiency of full-duplex-based handshaking, [22] proposed a full-duplex collision avoidance (FDCA) MAC protocol, in which collisions are prevented through a transmission scheduling algorithm based on the propagation delay information of neighboring nodes. With FDCA-MAC, a transmitter launches multiple simultaneous handshaking processes with its neighbors to propagate multiple packets concurrently. However, this protocol requires accurate time synchronization and does not address the exposed terminal problem. Similarly, [23] proposed a two-fold handshaking full-duplex MAC protocol (THFD-MAC) that exploits multiple transmissions with one handshake, where concurrent transmissions are scheduled and received by the sink node.

Recent studies have shown that directional communication technology can significantly improve network performance by suppressing interference. [24] proposed a dual-sensing directional MAC (DSDMAC) protocol to address the deafness problem. In DSDMAC, a non-interfering out-of-band busy tone signal combined with the detection of activity on the actual data channel is used to identify deafness situations and avoid unnecessary blocking. However, dual-sensing is capitalized on a single antenna. It is infeasible for underwater acoustic transducers to transmit the omnidirectional busy-tone and receive the directional data simultaneously. Furthermore, a predetermined neighbor table is required for the protocol.

To distinguish deafness from data collisions, [25] proposed a deafness-aware MAC (DA-MAC) protocol, in which different responses for the transmitted RTS packets on two independent logical channels were utilized, and a multibeam antenna system was adopted. Each beam could be controlled independently; thus, omnidirectional transmission and reception abilities are available, along with directional ability. However, the complexity of the antenna system makes it unsuitable for use in UASNs.

Directional communication can improve network performance by achieving spatial reuse. However, many of the solutions are based on the assumption that the network topology is known [24]–[26] or adopt an inefficient neighbor discovery algorithm [27], [28]. It is too time-consuming for nodes equipped with a single directional antenna to scan around to discover all neighbors [29]–[31], which is especially serious for UASNs with large RTTs. Therefore, an efficient neighbor discovery approach is required to improve network performance.

Motivated by these ideas, this study attempts to address the challenges and disadvantages of directional communication technology through full-duplex technology, making this the first study to attempt this approach. With the proposed framework, not only the problem of directional neighbor discovery is addressed, but also the challenges caused by impractical sensor systems [24], [25].

III. System Model

There are two available channels in our proposed framework: the primary channel (in the higher-frequency band) and the secondary channel (in the lower-frequency band). The vector hydrophone that works in the secondary channel is used to estimate the direction of overheard arrivals; thus, consequent action strategies (neighbor table update, silence or not, which will be discussed later) could be adjusted in time. The multimodal transducer can transmit and receive in both channels.

TABLE I
Operation Modes of the Sensors

Type		Vector Hydrophone	Modal Transducer
Center Frequency	15kHz	✓	✓
	25kHz	×	✓
Directivity	O	✓	✓
	D	×	✓
Role	Receive	✓	✓
	Send	×	✓

O- denotes the omni-directional capability and D- denotes the directional capability.

To achieve these, we made the following assumptions on the system architecture:

- A node has two independent sensors: a vector hydrophone and a multi-modal transducer.
- A vector hydrophone can only receive, whereas a multimodal transducer can both transmit and receive [32].
- There are two available frequency bands: the vector hydrophone works in a fixed lower band, whereas the multimodal transducer is free to choose either.
- The beam-forming mode of the multimodal transducer can be adjusted to be directional or omnidirectional. If the directional mode is chosen, only one sector can be activated at a particular time.

Based on the above assumptions, the operation modes of the sensors (vector hydrophone and modal transducer) are clarified, as shown in Table I:

In addition, the communication and energy consumption models are defined based on the above analyses.

A. Directional Modules in UASNs

1) Vector Hydrophone: A vector hydrophone, composed of an omnidirectional sound pressure sensor and three particle velocity sensors that are perpendicular to each other, can measure the scalar acoustic pressure along with the acoustic particle velocity (motion or acceleration) [33]. Consider a two-dimensional Euclidean plane with an underwater acoustic field. The sound field parameters are given by [34]

$$p(t) = s(t) \tag{1a}$$
$$v_x(t) = s(t)\cos\theta \tag{1b}$$
$$v_y(t) = s(t)\sin\theta \tag{1c}$$

where $s(t), \theta$ denote the sound pressure and spatial azimuth of a signal, and $v_x(t), v_y(t)$ denote the orthogonal velocity components in the plane. Thus, the integrated velocities $v_h(t)$ and $v_s(t)$ are derived by combining the two components in the plane, as follows:

$$v_h(t) = v_x(t)\cos\phi + v_y(t)\sin\phi \tag{2a}$$
$$v_s(t) = v_x(t)\sin\phi - v_y(t)\cos\phi \tag{2b}$$

We obtain (3) by combining (1) and (2), as follows:

$$v_h(t) = s(t)\cos(\phi - \theta) \tag{3a}$$
$$v_s(t) = s(t)\sin(\phi - \theta) \tag{3b}$$

The symbol ϕ in (2) and (3) denotes the azimuth of the receiving directivity generated by the vector hydrophone. Thus, with $\phi = \theta$, the maximum directional gain for an arbitrary azimuth θ is obtained [35].

Furthermore, various directivity performances can be achieved by collocating different p and v, such as $p + v$, $p + 2v$, and $(p + v)p$. Among these, $(p + v)p$ provides the best directivity index $D_{p,v}$, as shown in (4), where C_0 denotes a normalized value, and $\tau = \phi - \theta$.

$$\begin{aligned} D_{p,v} &= (p(t) + v_h(t))v_h(t) \\ &= (s(t) + s(t)\cos(\phi - \theta)) * s(t)\cos(\phi - \theta) \\ &= s(t) * \cos\tau(1 + \cos\tau) \\ &= C_0 \cos\tau(1 + \cos\tau). \end{aligned} \tag{4}$$

The results show that a vector hydrophone provides both directivity and omni-directivity. These can be used to estimate the azimuth angle of a source node, which will be explained in the following section.

2) Multi-Modal Transducer: Based on the concept of generating beam patterns by exciting modal beam patterns in the surrounding acoustical fluid simultaneously along with specific weighting functions, a multimodal transducer can obtain the desired beam pattern through the superposition of the components operating in different modes. If we limit the beam pattern to the first three modes [36], the beam-pattern pressure function $p(\theta)$ can be expressed as

$$\frac{p(\theta)}{p(0}) = \frac{A_0 + A_1\cos\theta + A_2\cos 2\theta}{A_0 + A_1 + A_2} \tag{5}$$

where θ is the beam pattern angle and A_i is the weighting function for the ith operating mode normalized by $A_0 = 1$.

Therefore, the appropriate parameters for A_1 and A_2 can be selected to obtain the required directivity performance. Recall the receiving directivity index denoted by (4). The formulation can be further simplified as

$$\begin{aligned} D_{rec} &= C_0\cos\tau(1 + \cos\tau) \\ &= C_0(\cos\tau + \cos^2\tau) \\ &= C_0(\cos\tau + \frac{1 + \cos 2\tau}{2}) \\ &= C_0\frac{1 + 2\cos\tau + \cos 2\tau}{2}. \end{aligned} \tag{6}$$

The normalized transmission directional index is equal to the reception directional index, under the condition that $A_1 = 2$, $A_2 = 1$, and $C_0 = 1/2$, implying that identical transmission and reception directivity indices can be provided within the framework, which ability contributes significantly to reducing the complexity of the upper-layer protocol design.

Consequently, the corresponding -3 dB directional beam width can be obtained at approximately 76°. Finally, a steerable beam system for UADSNs is established, where the entire coverage area is divided into six sectors, each of which can be activated by adjusting the multimodal transducer.

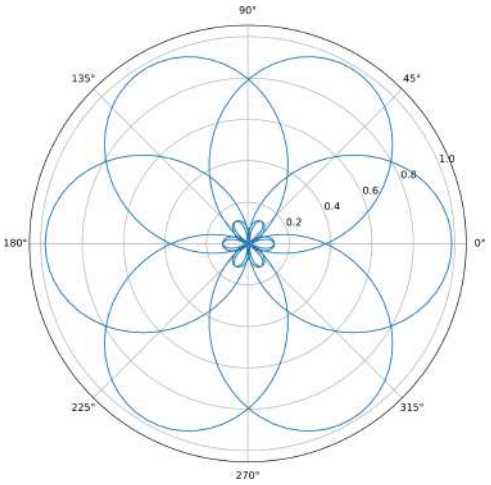

Fig. 1. Joint directivity index diagram of the steerable beam system.

The joint directivity index diagram is shown in Fig. 1, which is simplified as a pie diagram with a sectorial beam-width of $\pi/3$ in this study for convenience.

B. Communication Model

In an omnidirectional network, nodes can communicate as long as they are located within the communication range of each other. This type of network is often represented by a unit disk graph(UDG), where the communication mode of omnidirectional transmission with omnidirectional reception (OO) is adopted. Its advantage is easier coordination between the communicating nodes, but it suffers from more power consumption. Alternatively, a pair of nodes in a directional network could communicate only when they are located in each other's active beam, that is, their beams have to steer toward each other. This communication mode is called directional transmission with directional reception (DD), which saves energy and reduces interference but needs complicated pre-coordination. Another mode, i.e., directional transmission with omnidirectional reception (DO) or vice versa (OD), has advantages in trading off the system complexity and power efficiency. The comparison of the three communication modes is shown in Fig. 2.

In this paper, all the three modes are flexibly adopted for collaborative work, depending on the communication purpose, to make full use of their advantages, which will be described below.

C. Energy Model

This section discusses the energy efficiency achieved by the proposed directional transducer model and derives a theoretical energy model for the directional modules.

As is known, the sound intensity I on a beam surface is expressed as

$$I = \frac{W_p}{S} \tag{7}$$

where W_p denotes the sound power, S denotes the surface area [37] and $W_p = IS$, indicates that the sound power is proportional to the surface area covered by a beam.

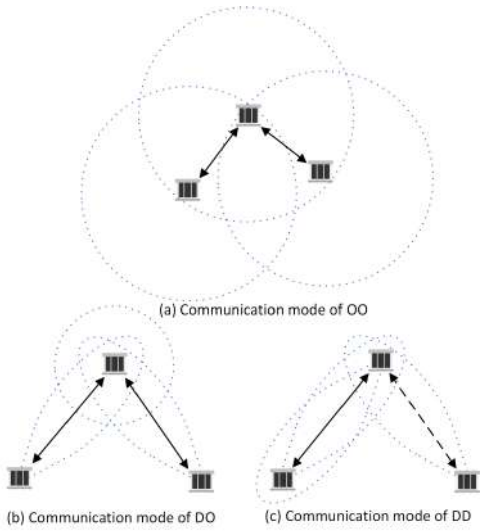

Fig. 2. Visualization of the three types of communication modes. (The solid line with bidirectional arrows denotes a valid link between two nodes, whereas a dashed line indicates the two nodes can not communicate).

In addition, the sound intensity has a numerical transition with the sound pressure, as shown below [38]:

$$I = p^2/\rho c \tag{8}$$

where p denotes the sound pressure of a beam and the product ρc denotes the acoustic impedance of the transport medium.

Without loss of generality, let $\rho c = 1$, we can obtain

$$\begin{aligned} I(\theta) &= p^2(\theta) \\ &= (\frac{1 + 2\cos\theta + \cos 2\theta}{4})^2 \\ &= \cos^2\theta \cos^4\frac{\theta}{2} \end{aligned} \tag{9}$$

for the adopted beam-form pattern of $A_1 = 2, A_2 = 1$ ($p(0)$ in (8) is a reference sound pressure that regarded as 1), by combining (8) and (5).

Considering the transmission in 3D space, if conversion loss is ignored and the maximum propagation range of a beam is fixed, the energy consumption can be characterized by the surface area at which the sound intensity is identical. Let us denote the energy consumption by C_m, where $m \in \{D, O\}$ denotes the communication mode.

Given that the surface of a revolution in polar coordinates can be expressed as [39]:

$$S = 2\pi \int_{\alpha}^{\beta} \rho(\theta)\sin(\theta)\sqrt{\rho^2(\theta) + [\rho'(\theta)]^2}\mathrm{d}\theta. \tag{10}$$

We can obtain the surface area of a beam that represents the energy consumption. Thus, the energy consumed by the directional communication C_D can be obtained by substituting $\rho(\theta)$ in (10) with (9). As the solution of C_D is not available in closed-form, we used a numerical integration method for the estimation; finally, $C_D \approx 1.77$ was obtained for $\alpha = 0, \beta = \frac{\pi}{2}$.

For the omnidirectional transmission, C_O is easy to calculate using the formula of unit sphere surface area, which is $4\pi \approx 12.57$. Based on the analyses, we defined a metric of the energy efficiency ratio (EER) for further evaluation:

$$EER_D^O = \frac{C_O}{C_D} = 7.1. \tag{11}$$

This means that, compared with omnidirectional transmissions, directional transmission saves approximately $(7.1 - 1)/7.1 = 85.9\%$ energy through the communication mode of DO. The value further increases if the communication mode of DD is used because symmetrical directional gains are available for both directional transmission and reception.

Furthermore, if the sound power is fixed, according to (7) we have:

$$I_D = W_D/S_D \tag{12a}$$

$$I_O = W_O/S_O \tag{12b}$$

where I_D, I_O denote the sound intensity of a directional and an omnidirectional beam, respectively.

Thus, the ratio of the transmitted radiant intensity in a specified direction to the radiant intensity transmitted by an isotropic radiator is obtained as $I_D/I_O = S_O/S_D$, resulting in a calculation for the on-axis directivity index in decibels as

$$\begin{aligned} DI &= 10\log(\frac{I_D}{I_O}) \\ &= 10\log(EER_D^O) \\ &= 8.5. \end{aligned} \tag{13}$$

The result indicates that a DI of 8.5 dB is gained for the beamwidth of 76°, which is very close to [36], proving the model's accuracy.

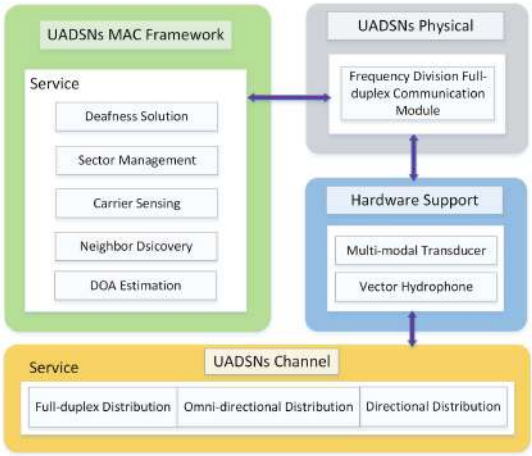

Fig. 3. The proposed MAC framework.

IV. Description of the Proposed Framework

In the proposed MAC framework, comprehensive services required for UADSNs are presented, as shown in Fig. 3.

Notably, the MAC framework provides several pivotal services based on the independently equipped vector hydrophone and multimodal transducer, contributing to the MAC protocols working well. The physical layer and channel modeling are not discussed as they are beyond the scope of this paper.

A. Direction of Arrival Estimation

The geographical locations of the neighbors in UASNs are challenging to acquire, which issue is more severe for UADSNs but can be addressed through a vector hydrophone capable of estimating the direction of arrival (DoA) [40]. In the proposed framework, a node does not need to know the accurate azimuths of its neighbors; therefore, the average sound intensity estimation(time-domain approach) is used to estimate the DoA using a single vector hydrophone [41]. The measured particle velocity of a target located at P in the 2D plane is denoted by

$$\mathbf{v}(t) = \mathbf{i}v_x(t) + \mathbf{j}v_y(t) \tag{14}$$

where the relationship between the particle velocity and its components is shown in (1). Thus, the vector sound intensity is

$$\boldsymbol{I} = p(t)\mathbf{v}(t). \tag{15}$$

Substituting (15) with (14), we get:

$$\boldsymbol{I} = \mathbf{i}I_x(t) + \mathbf{j}I_y(t). \tag{16}$$

The horizontal azimuth is obtained by combining (16) and (1) as

$$\phi(t) = \tanh \frac{I_y(t)}{I_x(t)}. \tag{17}$$

Consequently, the direction of arrival of an incoming packet can be estimated, which is a technically feasible assumption of the proposed framework.

B. Neighbor Discovery

In UASNs, neighboring node information is sometimes necessary for upper-layer protocols to perform better. A common method for establishing a neighbor table is collaboration-based [10], where a dialog is launched by a node that wants to know its neighbors. Once the neighbor receives the inquiry, it sends back a reply to notify the initiator of its MAC address.

This simple type of ND protocol is sufficient for general UASNs; however, it is unavailable for UADSNs as nodes in UADSNs, generally equipped with a directional transceiver, have to gather the MAC addresses and directions of neighbors.

A common ND protocol for directional sensor networks is based on sector sweeping; specifically, a node traverses all its beam sectors in a stochastic or predetermined manner to discover its neighbors, as 802.11ad [42] does. Nevertheless, this method requires too many RTTs and is difficult to converge; thus, it is unsuitable for underwater environments.

In the proposed framework, the ability to estimate DoA is provided by an extra-equipped vector hydrophone; hence, cooperation with a multimodal transducer could help discover all the potential neighbors under reasonable time constraints.

C. Carrier Sensing

Carrier sensing (CS) technology was initially used in WSNs for collision avoidance, where a node delays transmission for a period to sense the channel. There are two approaches to achieving this: (a) physical carrier sensing (PCS) and (b) virtual carrier sensing (VCS). PCS senses the channel using algorithms running in the physical layer, such as energy threshold judgment, whereas VCS achieves the goal through a network allocation vector (NAV) [43]. With NAV, the information of the estimated time to occupy the channel is included in the RTS/CTS packet; thus, a neighbor receiving the packet defers its transmission for the corresponding time, and the purpose of collision avoidance is obtained.

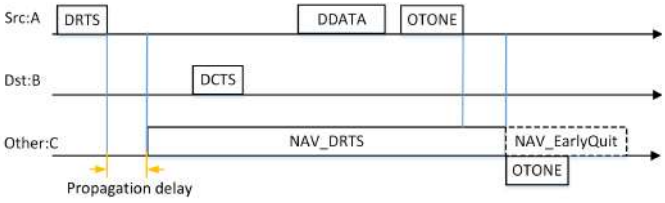

Fig. 4. The mechanism of directional CS.

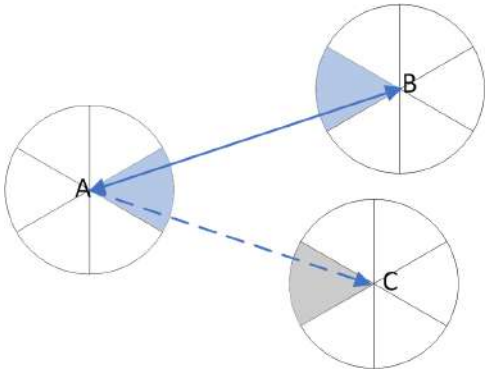

Fig. 5. Node *C* has to back-off in the grey sector.

In this framework, both approaches, directional PCS (DPCS) and directional VCS (DVCS) are available. With DPCS, a node will delay its transmission if it receives a control packet and realizes that it may interfere with the ongoing transmission. With DVCS, the node schedules its silence timer according to the NAV stored in an overheard control packet for the sector in a back-off state and quits the silence early once a warning is received.

The relevant mechanisms of directional CS are explained below in Fig. 4.

D. Sector State Management

For a node equipped with a single transducer, the state of the transducer (which determines whether a transmission is available) should always be noted. However, a steerable beam system must follow the state of each sector to prevent collisions during ongoing communication.

This is achievable for the proposed framework, which is equipped with an extra vector hydrophone that overhears the surroundings and updates the states for every captured event. When bound with a timer, each sector remains silent unless it is scheduled to be activated. Therefore, interference in this direction is avoided, and other sectors are not affected.

A sector can be used for transmission and reception only when active. As shown in Fig. 5, node A receives an RTS

TABLE II
THE NOTATIONS USED IN THE FDD-MAC

Type	Communication Model	Objective	Frequency (kHz)
OHELLO	OO	Neighbor discovery	15
DRTS	DO	Request to send	15
DCTS	DO	Clear to send	15
DATA	DD	Data transmission	25
OACK	OO	Acknowledgement &Reduce deafness	15
OTONE	OO	Reduce deafness	15

O- denotes an omnidirectional packet and D- denotes a directional packet.

from B. Thus C, also covered by the same sector as A, has to back off in the gray sector to avoid collisions in this direction because it is now a hidden terminal. Conversely, if A initializes a dialog and C receives the RTS, the gray sector of C cannot be used for receiving, but is available for sending.

The node must estimate the back-off time depending on its role and the packet it receives in this process. For a transmitter that behaves as an exposed transmitting terminal, it has to keep silent in the sector where a DCTS is received, for at least $3 * T_d + T_D + 2 * T_C$, where T_d, T_D, T_C denotes the maximum propagation delay, the transmission time of the data packet and the control packet, respectively. However, for a receiver, it has to back off in the sector where a DRTS is received, as the sector would be subsequently interfered for at least $4 * T_d + T_D + 3 * T_C$. The reason for the different back-off time can be learned from Fig. 4 that, an overheard DRTS implies the following three handshaking processes: two control and data packet transmissions, where a guard interval equal to $T_d + T_C$ is considered to avoid collisions. However, an overheard DCTS implies the following two handshaking processes: a control packet and a data packet transmission.

E. Deafness Solution

As an induced problem of a network using a single directional transducer, the deafness problem [44] occurs when a node S_1 wants to send a packet to a sink R, while R is communicating with another sender S_2. In this situation, sink R must beam-form its direction to S_2, so it cannot overhear the latter's request. As a result, S_1 is unaware of the reason leading to no reply, and its back-off time may increase rapidly.

Therefore, a mechanism called early warning is provided in the framework to address the problem of deafness, where a node can notify the neighbors of a finished dialog. Specifically, a node broadcasts a short notification packet once its transmission ends, preventing its neighbors from becoming deaf. In this way, the deafness effect is minimized, as shown in Fig. 4, where a node in long silence recovers once it receives the corresponding omnidirectional notification.

V. PROTOCOL DESIGN

In this section, an asynchronous contention-based FDD-MAC protocol is elaborated to exploit the advantages of the proposed framework. To clarify this description, we list the notations used in the following section in Table II.

In the table, each packet Pkt is expressed as $Pkt_{dst}(frq)$ to indicate the destination dst and transmission frequency frq in Hz, where the communication mode and packet source are implied.

A. FDD-MAC Overview

The protocol consists of three phases: neighbor discovery, channel reservation, and data transmission. The neighbor discovery phase is used to discover as many neighbors as possible in a positive method. The channel reservation phase is used to contend the channel by handshaking. Once the channel is reserved, the data transmission phase begins, where an efficient method of data train is adopted to further improve the network performance.

1) Neighbor Discovery: To build local neighbor maps for sparse UADSNs, we propose a simple but efficient neighbor discovery method using one vector hydrophone. The main idea is a two-phase joint neighbor discovery strategy, which includes a process of proactive neighbor discovery and a process of passive neighbor update and maintenance. The former approach, launched periodically, provides a starting condition, whereas the latter will be launched after the network is set up, assisting failure-link recovery.

Specifically, in the process of proactive neighbor discovery, a node sends an OHELLO packet n times by a multimodal transducer without ACK. This strategy is based on the observation that the OHELLO packet consists of two MAC addresses, which are no more than six bytes and can be lower if a particular address format is used. The transmission and reception times of the OHELLO packet are in the order of 10^{-2}s for a physical data rate of 2000 bps, which is sufficiently small compared with the propagation delay. However, if a reply for OHELLO is adopted, each node must send at least one OHELLO and reply N_i times (N_i is the number of neighbors of node i). Even though, it does not contribute to a higher discovery probability, as the OHELLO is sent by broadcast, once a collision occurs, the receiving node cannot distinguish the OHELLO from which it is dropped, and a repeated discovery process may be required, which wastes much energy and time, thus becoming inefficient.

According to the network scope, n is selected to be three intuitively to improve the discovery probability. The transmissions of the OHELLOs are launched within a random period after the network is initialized. The interval between two adjacent transmissions is also stochastic. Thus, all the OHELLOs of an ND phase can be sent within an RTT. As long as any of the transmitted OHELLOs are received by the neighbors, a table entry mapping the MAC address, corresponding azimuth, and beam sector identification is established.

Furthermore, in case all the OHELLOs are lost or the topology changes, the process of passive neighbor update and maintenance is launched after the network works. Each neighbor table entry has a survival time which is updated whenever a packet is overheard in the following process (any packet received indicates that its source node is located in the communication range). In this way, an old inactive neighbor is invalidated, and a new one is cached in time.

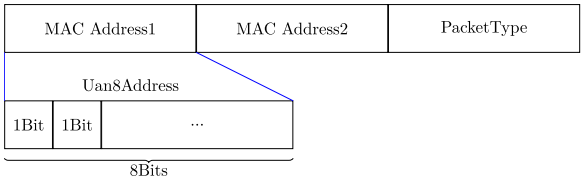

Fig. 6. Packet format of OHELLO.

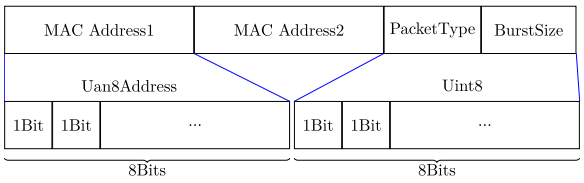

Fig. 7. Packet format of DRTS.

In this study, a specialized 8-bit address format for MAC, Uan8Address, is adopted. The format of OHELLO is shown in Fig. 6. Up to 255 unique nodes can be accommodated using 8 bits, sufficient for current underwater network research.

2) Channel Reservation: The channel reservation phase begins as soon as the neighbor table is established. In the phase, a handshaking process is launched to improve the spatial reuse and solve the hidden/exposed terminal problem. A node with packets to deliver first enqueues the arrivals and sends a DRTS to its communication peer dst in the directional mode. Considering that the DRTS is sent without prior knowledge of the orientation of the peer's multimodal transducer, its destination entry must be the vector hydrophone. Thus, the frequency band used should be in agreement with the vector hydrophone, and the DRTS format is $DRTS_{dst}(15k)$.

A DRTS transmission has two purposes. First, it informs the receiver of the following data stream so that the intended receiver can adjust its multimodal transducer (i.e., the beam direction) in time. Second, it carries the NAV of the data that will be transmitted to reserve the channel, which stores the MAC addresses of the sender and receiver and the packet type and length of the incoming packet train (termed as $BurstSize$ and used for calculating NAV). The DRTS format is shown in Fig.7, where the fields of $PacketType$ and $BurstSize$ are four higher and four lower bits, respectively, sharing a single uint8 data type. Thus, the maximum packet size was limited to $2^4 = 16$.

Once a DRTS is successfully received and its destination address matches, a DCTS, whose format is the same as the DRTS but the field of $PacketType$ differs, is sent back directionally at a frequency of 15kHz to inform the sender to send. Otherwise, the receiver will remain silent. Note that the sender continues orienting towards the direction of the DCTS and working at a frequency of 15 kHz, and may receive duplicate DCTSs, and the DCTS received at the vector hydrophone will be dropped.

In this way, a subsequent busy period in the direction is implied; thus, potential conflicts in the primary channel are prevented.

3) Data Transmission: The data transmission phase aims to improve channel utilization, which can be expressed as (18) for a typical handshaking process.

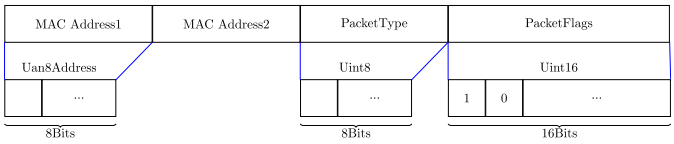

Fig. 8. Packet format of OACK.

$$R_u = \frac{l_D}{l_R + l_C + l_A + l_D + 2l_P} = \frac{1}{1 + \frac{l_R + l_C + l_A + 2l_P}{l_D}} \tag{18}$$

where l_R, l_C and l_A are the lengths of the RTS/CTS/ACK packets, respectively, and l_D is the length of the DATA packet. Without losing generality, the transmission time of the packets can be represented by the length. Therefore, we can see from (18) that if the distance l_P of a communicating pair is fixed, the channel utilization can be effectively improved by increasing l_D. A common method to increase l_D is to aggregate several packets. However, the packet error probability will rise rapidly with an increase in packet length [45], and subtle demodulation errors will cause the entire aggregated packet to be retransmitted.

Therefore, a method to transmit the packets one by one is adopted in the paper, i.e., data train (DT). A DT is sent once the DRTS has been replied, where a short guard interval exists between two successive packets to deal with the multipath effect.

Although the packet buffer of a node storing the arrivals may increase during the period when the node attempted to reserve the channel, it cannot send more packets than it reserved through the previous DRTS. Otherwise, the packets might be missed because the receiver may turn toward other senders.

The transmission of DT is followed by an early tone (termed OTONE, whose format is the same as that of OHELLO) to address the deafness problem, which is broadcasted as $OTONE_B(15k)$, where B denotes the broadcast address.

In addition, another measure to further improve the solution to the deafness problem is introduced at the sink, i.e., it broadcasts an OACK to inform the neighbors of its idle state after the reception of DT. The OACK has the format $OACK_B(15k)$, so it does not affect the data transmission.

In the design of OACK, a mechanism of aggregation is used to shorten its length, thus saving energy. Specifically, a received packet is denoted by an ordered bit in the $PacketFlags$ field, as shown in Fig. 8. where the values 1 and 0 indicate that the first received packet is correct, whereas the next packet is not demodulated successfully.

Considering that the limit on the length of a packet train is 16, an uint16 data type is used to store the flags. Therefore, the node receiving the specialized OACK can recover the reception status of the transmitted packets and drop the successfully received packets from the packet queue maintained for packets that need to be retransmitted. A packet remains in the queue until it is successfully received or the number of retransmissions exceeds the limit. Eventually, if the OACK is

missed, a node must re-contend the channel, as most MAC protocols do.

B. Power Control Algorithm

In addition to the basic principles stated above, a novel rough power control algorithm is developed to make FDD-MAC work better.

As illustrated in Section III-A.2, the directional transducer exhibits the same DI performance as the vector hydrophone. The DI in different azimuths varies and can be calculated. Considering that there is no handshake in the ND process, a distance estimation algorithm based on time difference is unavailable; however, the signal strength information can be used as a foundation of the power control strategy.

In a network, only the signal-to-noise ratio (SNR) of a signal could be obtained at the receiver. Furthermore, if all nodes are homogeneous, the maximum source level provided, SL_{max}, is identical (this assumption is reasonable, as the source level has a simple transition relationship with the transmission power). Thus, according to the passive sonar equation [37], we get

$$\begin{aligned} TL &= SL_{max} - NL - SNR \\ TL &= SL_{min} - NL - TH \end{aligned} \tag{19a}$$

where NL and TL denote the ambient noise level and transmission loss in dB re μPa, and TH denotes the threshold to demodulate a packet successfully.

Although NL consists of multiple components, it is unnecessary to calculate them because the links between two peer nodes are approximately symmetric. In this way, an adaptation method to estimate the required minimum source-level SL_{min} is obtained according to (19):

$$SL_{min} = SL_{max} - SNR + TH. \tag{20}$$

The results demonstrate a power control strategy without directional Tx/Rx. For directional Tx/Rx using different communication modes, it is easy to calculate DI if the azimuth is known (the process is detailed in (5)). Thus, the transmission powers for the different communication modes are obtained according to (20):

$$SL_{OO} = SL_{max} - SNR + TH + SL_o \tag{21a}$$

$$SL_{DO} = SL_{max} - SNR + TH - DI + SL_o \tag{21b}$$

$$SL_{DD} = SL_{max} - SNR + TH - 2DI + SL_o \tag{21c}$$

where the symbol SL_o, in dB re μPa, denotes the source level offset needed for different transmission modes (frequency and bandwidth) to reach the same distance, which can be pre-determined before the network is configured. In this process, the characteristic of the underwater channel that an acoustic signal in lower frequency attenuates slower than that in higher frequency is considered.

Eventually, self-adaptive power control strategies were established, which can be achieved through the ND process of the proposed framework.

C. States of Sectors

Although the framework greatly minimizes mutual interference among nodes, collisions cannot be eliminated. Each node maintains a sector state manager (SSM) that manages the state of each sector to ensure interference-free communication. A sector has three working states, i.e., *IDLE* (can transmit/receive), *NOTX* (can only receive), and *NORCV* (can only transmit with a modal transducer). The state is updated passively according to the packets the vector hydrophone overhears. In case of the long time unnecessary back-off, the expiration time for the *NOTX* and *NORCV* states are scheduled after delays $3 * T_d + T_{DT} + 2 * T_C$ and $4 * T_d + T_{DT} + 3 * T_C$, respectively, according to the analysis in Section IV-D, where T_{DT}, carried in the NAV, denotes the time used to transmit the reserved data train.

In summary, with our proposed protocol, a sector needs to back off in the following cases:

- An xDRTS is overheard by a receiver, or an xDCTS is overheard by a transmitter, whose destination node is located in the beam range of the sector. The back-off time follows the principles discussed above.
- A transmission failure occurs in the sector, followed by retransmission.
- Every successful transmission is followed by a short random back-off period to conduct DPCS to avoid collisions and acquire fairness in channel access.

In this way, potential collisions are avoided, and parallel transmissions are allowed.

D. Addressing the Exposed Terminal Problem

In FDD-MAC, the exposed terminal problem can be handled well due to the power control ability and directional communication technology.

Benefiting from the extra advantage brought about by ND, a node can easily decide if it becomes an exposed terminal through a local neighbor table. It will back off in a sector where ongoing transmission may interfere. However, the consequent behavior will not be halted if the intended destination is beyond its range (it does not exist in its neighbor table). This process is illustrated in Fig.9.

As can be seen, if node C (which is covered by a beam of A) has initialized a dialog, it will not interfere with the reception of B, although it is an exposed transmitting terminal for B, its beam is restricted. Meanwhile, B is an exposed receiving terminal for C; however, transmission from A cannot disturb D's reception for the same reason. In this way, the exposed terminal problem is completely addressed.

At last, a Markov state (which takes the state of sectors into consideration) transition diagram of the entire proposed protocol is shown in Fig. 10.

VI. Evaluations

In this section, we evaluate the performance of FDD-MAC in terms of ND efficiency, channel utilization, end-to-end delay, and energy consumption (efficiency). The results from our proposed approach were compared with those of some classical MAC protocols, such as UW-Aloha [46], S-FAMA [11], and UW-SEEDEX [47].

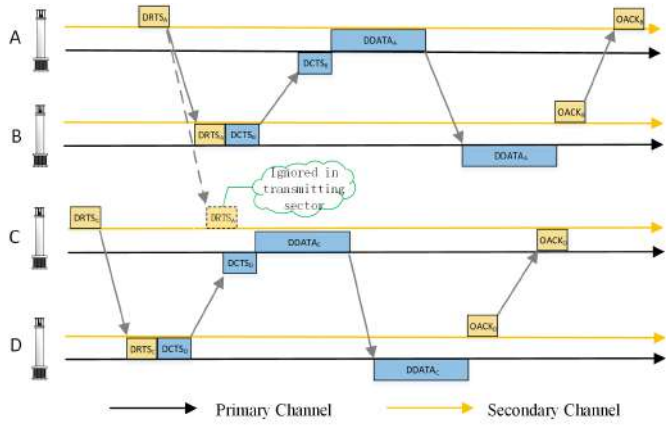

Fig. 9. The exposed terminal problem is addressed in FDD-MAC (a packet above the line indicates it is transmitted on the channel, otherwise received).

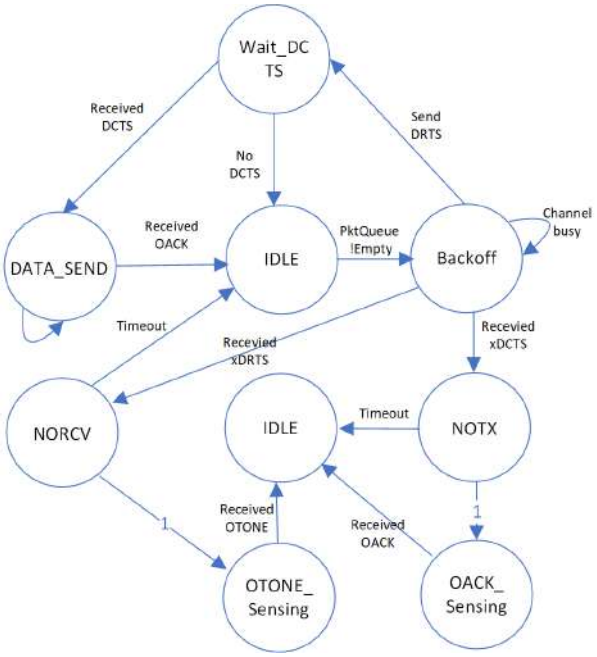

Fig. 10. State transition diagram for a sector in FDD-MAC.

A. ND Efficiency

To evaluate the efficiency of the ND algorithm in FDD-MAC for different network densities, we define a metric of the neighbor discovery ratio (NDR) as (22). The nodes are uniformly distributed in a 2D square region with a side length of 5000 m, the size of the OHELLO is 24 bits, and the physical data rate is 2000 bps. The transmission range of the nodes was 1250 m, and no decoding error was assumed during the process.

$$NDR = \frac{\sum\limits_{\forall i \in V} ND_i}{\sum\limits_{\forall i \in V} N_i}. \tag{22}$$

Here, ND_i denotes the number of discovered neighbors by an arbitrary node i, and N_i denotes the actual number of neighbors of node i. The NDR achieved using the proposed method is shown in Fig.11.

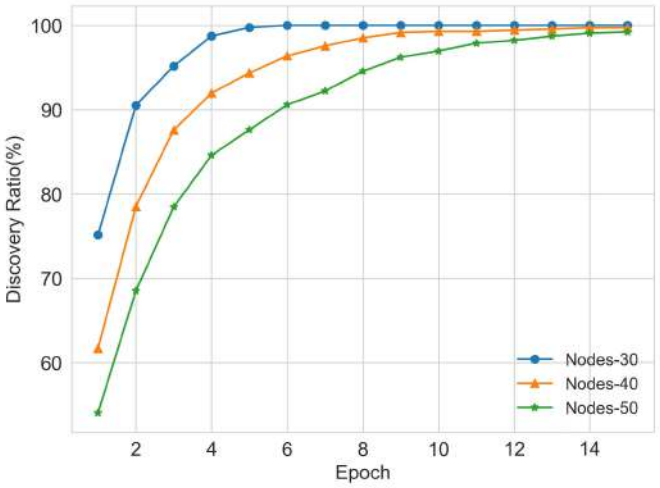

Fig. 11. Performance of NDR in random topology.

TABLE III
SIMULATION PARAMETERS OF THE NETWORKS

Parameter	Network Type	
	UASNs	UADSNs
Range (m)	4000	4000
SINR Threshold (dB)	10	10
Packet Size (bytes)	256	256
Traffic Rate (bps)	50-400	50-400
Data Rate (bps)	2000	2000
Band Frequency (kHz)	25	25,15
Bandwidth (kHz)	5	5,2
TxPowerW (W)	50	7.04

As shown in Fig. 11, in a sparse network, the ND protocol is efficient, with a discovery ratio of 90% achieved within two epochs. In fact, the protocol performs better for large ranges because a larger sending window further alleviates collisions.

B. Protocol Performances

1) Simulation Setup: Two types of topologies are simulated in NS-3 [48] that is extended for UADSNs: (a) A chain network in which five nodes only communicate with their direct neighbors, as shown in Fig. 12(a). In this topology, the distance between two adjacent nodes is 1000 m, and the source nodes deliver packets to the sink. (b) A mesh network with nine fixed nodes, as shown in Fig. 12(b). Each sender randomly selects a sink within one hop for transmission.

For both scenarios, all nodes are assumed to be static after deployment, and the relevant global parameters for the simulation are listed in Table III. Meanwhile, the protocol parameters required to run UW-SEEDEX follow [47].

In addition, the maximum transmission power used for FDD-MAC was predetermined using the calculation principles given in [49]. To generate hidden and exposed terminals for a better comparison, we used a maximum transmission range of 1200 m for the chain topology and 3000 m for the mesh topology. For example, in the latter scenario, a maximum source level of $SL_{max} = 149.9$ dB is required for transmission on the

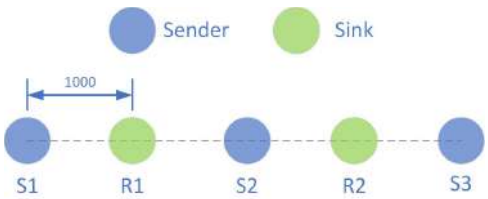

(a) Topology of the chain network.

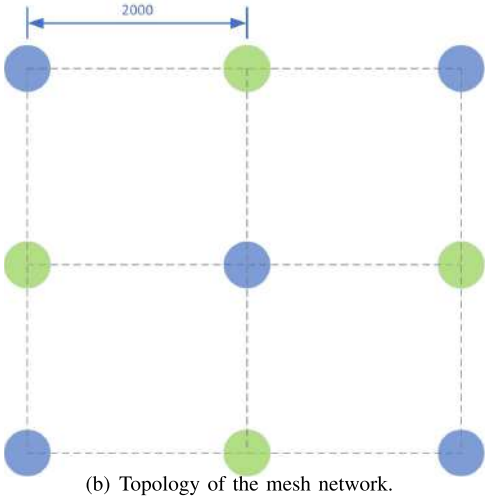

(b) Topology of the mesh network.

Fig. 12. The network topologies used for evaluation.

primary channel (frequency of $25k$) and $SL_{max} = 139.2$ dB for transmission on the secondary channel (frequency of $15k$). In this way, we obtain the source level offset of 4.1 dB and 10.7 dB for different scenarios, ensuring sufficient power for communications at the required distances.

In the simulations, each run lasted 2000 s, and an average value of 50 runs with a 95% confidence interval was counted. It should be noted that parameter $TxPowerW$ in Table III was used to trace the energy consumption of the network.

2) Simulation Results and Analysis: For the above multi-sink scenarios, we used the metric channel utilization ratio (CUR), which is defined as (23), instead of throughput to indicate the spatial reusability.

$$\begin{aligned} U_c &= \frac{T_{ep}}{T_{sim}} \\ &= \frac{T_h * T_{sim}/R_P}{T_{sim}} \\ &= \frac{T_h}{R_P} * 100\% \end{aligned} \tag{23}$$

where T_{ep} denotes the transmission time of effective packets (packets that are successfully received), T_{sim} denotes the simulation time, T_h expresses the throughput of the network, and R_P is the physical data rate.

The CUR comparisons of the four protocols are shown in Fig. 13 and Fig. 14, where B indicates the maximum $BurstSize$.

We can observe from Fig. 13 that the CUR performance of the FDD-MAC protocol in the chain topology increases with an increase in the offered load and outperforms the other two protocols with a good margin consistently for all data

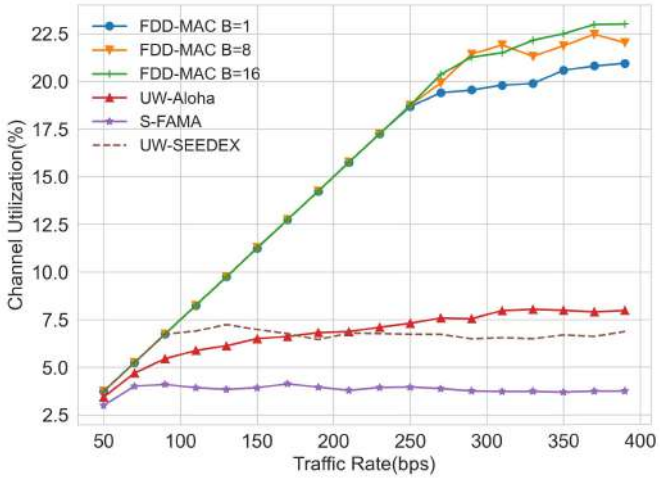

Fig. 13. Channel utilization of the chain networks using the four MAC protocols.

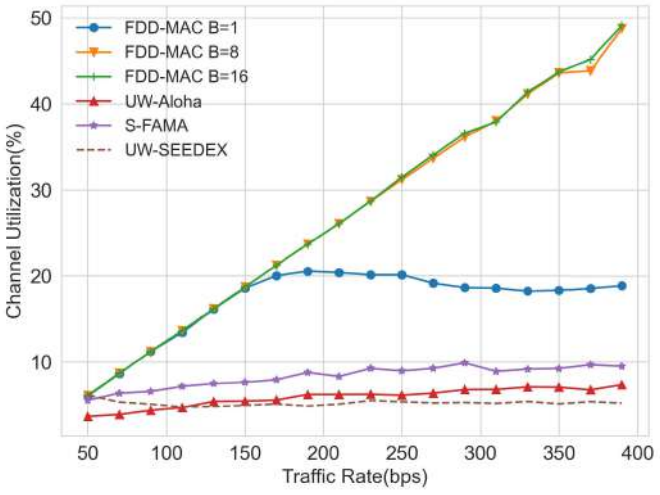

Fig. 14. Channel utilization of the mesh networks using the four MAC protocols.

rates. When $B = 1$, the curve tends to be stable and does not rapidly increase. However, the curves with $B = 8$ and $B = 16$ continue to increase with the traffic rate. Fig. 14 shows that the channel utilization of the FDD-MAC with $B = 1$ in the mesh network increases until a threshold is achieved; however, the situation is different for FDD-MAC with $B = 8$ and $B = 16$, as the delivery capability is still unsaturated. Meanwhile, the reference protocols achieve a much lower peak and saturation at an early stage. As can be seen, even when $B = 1$, FDD-MAC performs much better than UW-Aloha, S-FAMA, and UW-SEEDEX. This is because the directional beam focuses its energy and minimizes the interference.

To exploit the superior limits of the CUR performance of FDD-MAC, we conducted the simulations under a wider data rate scale from 100 to 2000 bps. The simulation parameters were the same as above, and each combination was run five times under different seed numbers. Finally, average results were obtained for both scenarios, as shown in Fig. 15 and Fig. 16.

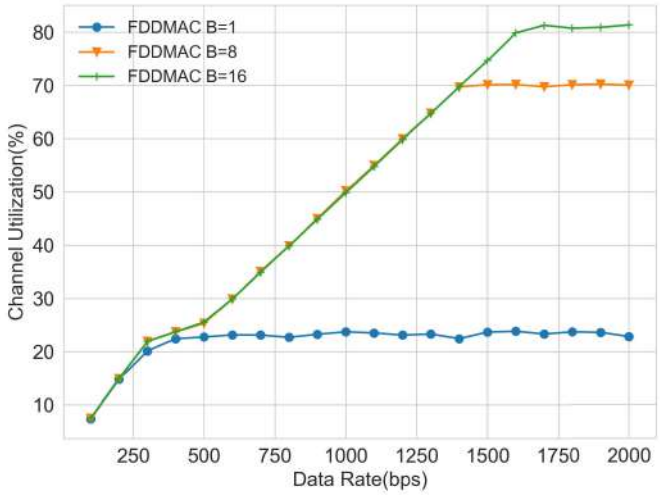

Fig. 15. Channel utilization of FDD-MAC in the chain network under a wider data rate scale.

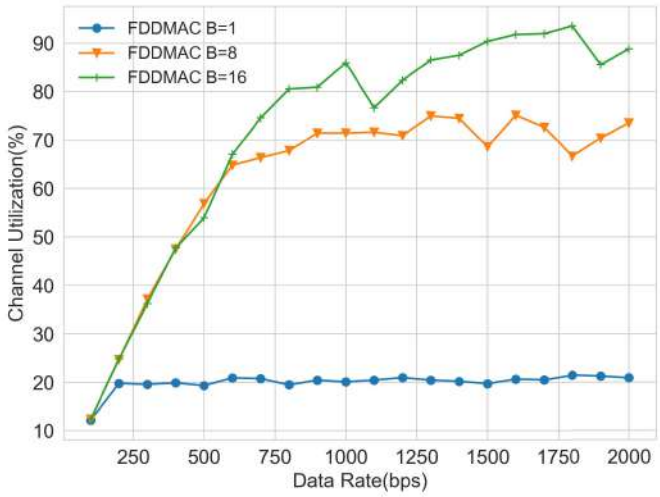

Fig. 16. Channel utilization of FDD-MAC in the mesh network under a wider data rate scale.

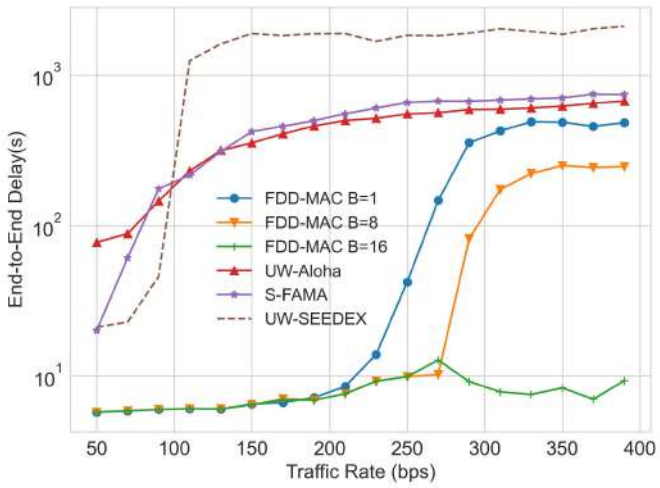

Fig. 17. End-to-end delay of the chain networks using the four MAC protocols.

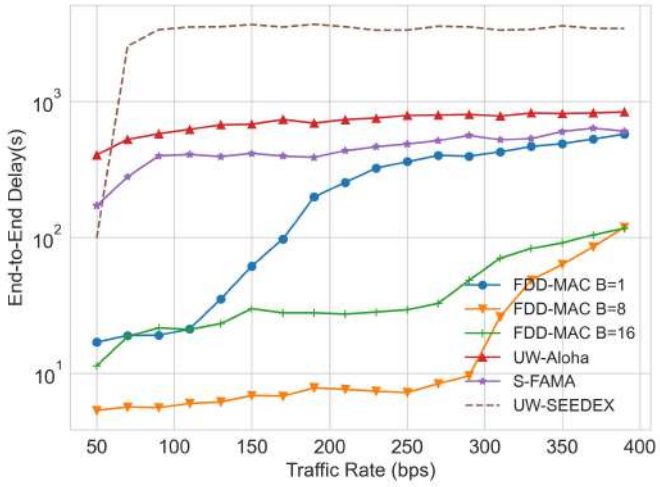

Fig. 18. End-to-end delay of the mesh networks using the four MAC protocols.

As depicted in the above figures, all the curves increase and remain stable after the data rate reaches a certain value. Benefiting from the mechanism of handshaking, the performance does not collapse with a continuous increase in the data rate. Eventually, CURs of up to 80% and 90% were achieved for the aforementioned topologies.

Fig. 17 shows the end-to-end delay of the four MAC protocols for the chain topology. The performance of the FDD-MAC with various $BurstSize$ remains low before the data rate reaches 250 bps and increases afterward, except for the situation when $B = 16$. This implies that the generated packets do not accumulate when the data rate is low. As can be seen, FDD-MAC outperforms the others even in the worst situation (i.e., $B = 1$).

A similar phenomenon was observed in the mesh network. We can see from Fig. 18 that FDD-MAC outperforms the compared protocols remarkably, along with the increase in traffic rate, owing to its spatial reuse capability (brought by directional transmission) and data training.

In addition, we provide a more comprehensive evaluation which is conducted for traffic rates from 100 bps to 2000 bps for both scenarios, as shown below in Fig. 19 and Fig.20.

Even when the traffic rate is very high, the proposed FDD-MAC achieves a much lower end-to-end delay than the control group in low traffic. Note that FDD-MAC performs better in the mesh scenario than in the chain scenario for two reasons: 1) the distances between senders and sinks in the mesh scenario are larger; 2) there are more destinations to determine for senders in the former case; thus, more competitions are introduced.

Fig. 21 shows the energy consumed by the MAC protocols in the chain topology. We can see that FDD-MAC saves more energy (nearly 80-90% of the compared protocols). This is owing to the energy-saving property of the directional communication technology of FDD-MAC. Fig. 22 shows the energy consumption in the mesh scenario. It can be seen that the energy consumption of FDD-MAC with $B = 8$ and $B = 16$ is higher than that with $B = 1$ after the traffic

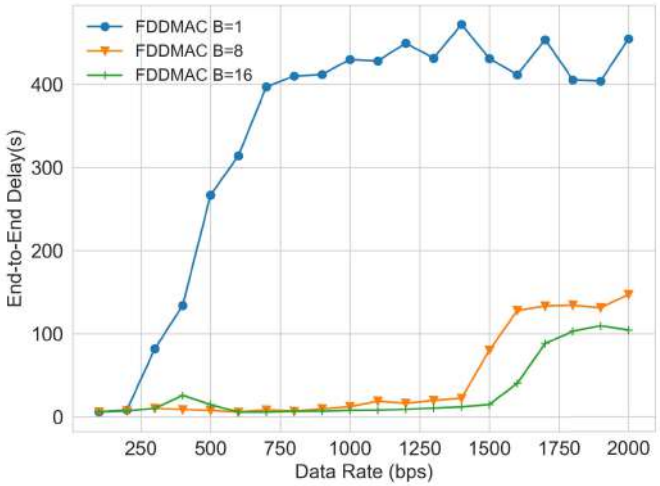

Fig. 19. End-to-end delays of FDD-MAC in the chain network under a wider data rate scale.

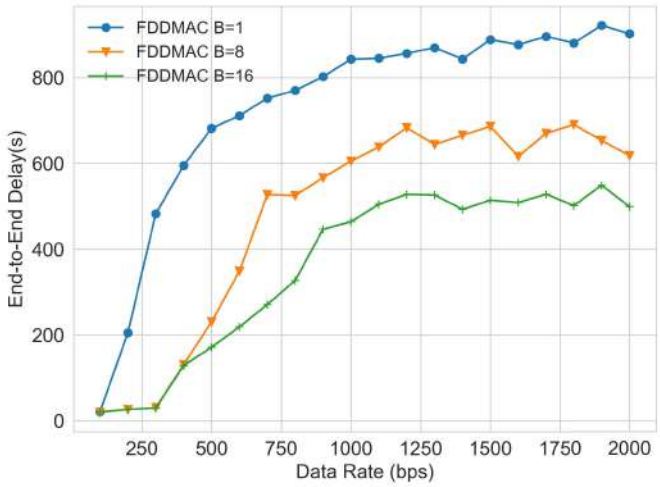

Fig. 20. End-to-end delays of FDD-MAC in the mesh network under a wider data rate scale.

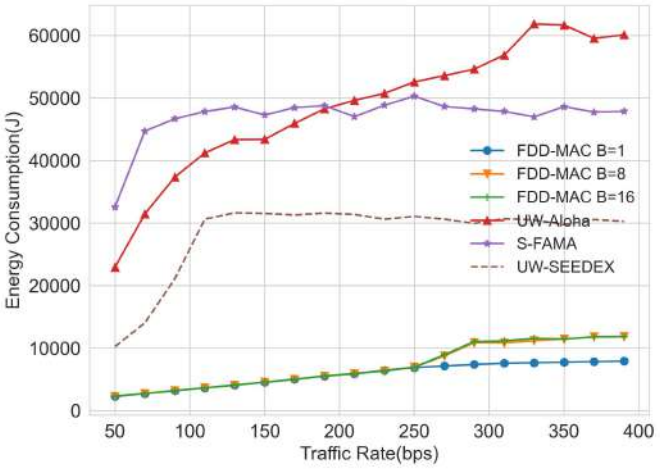

Fig. 21. Energy consumed by the chain networks using the four MAC protocols.

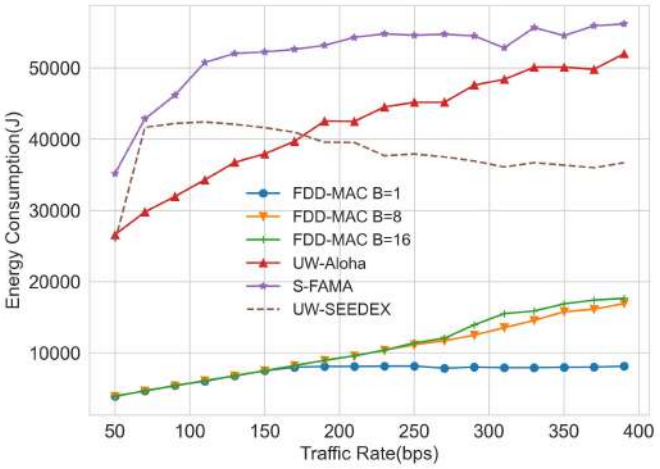

Fig. 22. Energy consumed by the mesh networks using the four MAC protocols.

rate exceeds 250 bps. This is owing to the high channel utilization (as a node transmits more packets in a particular period, as shown in Fig.13 and Fig. 14). From this discussion, we can also conclude that FDD-MAC achieves a high CUR while maintaining a low energy consumption.

Finally, the energy efficiency is defined as follows (24):

$$E_e = \frac{E_c}{B_r} \tag{24}$$

where E_c denotes the energy consumed during a period, and B_r indicates the data bits received. Thus, the metric characterizes the number of joules required to send a bit successfully on average. The energy efficiencies of the four protocols are shown in Fig. 23 and Fig. 24 for both topologies.

Fig. 23 and Fig. 24 indicate that FDD-MAC can access the channel with lower energy consumption with an increase in the traffic load. A slight decrease occurs early because the low traffic rate causes low $BurstSize$, reducing energy efficiency. Stable performance and an increase in the traffic rate demonstrate our proposed framework's good scalability, which

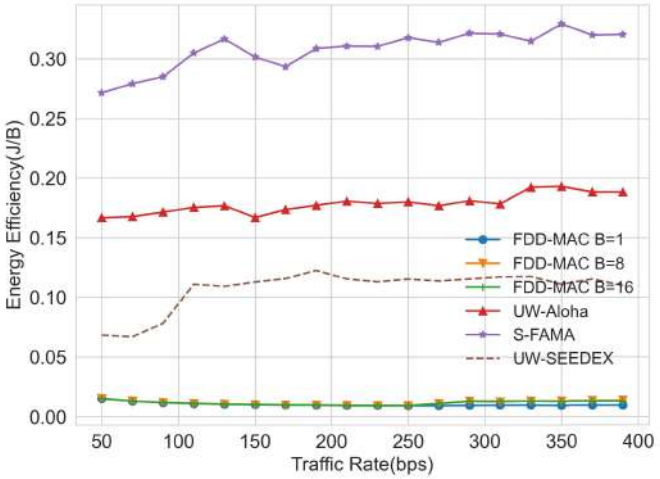

Fig. 23. Energy efficiency of the chain networks using the four MAC protocols.

is crucial for UASNs. Other protocols require higher costs to contend for the channel and retransmissions. A detailed

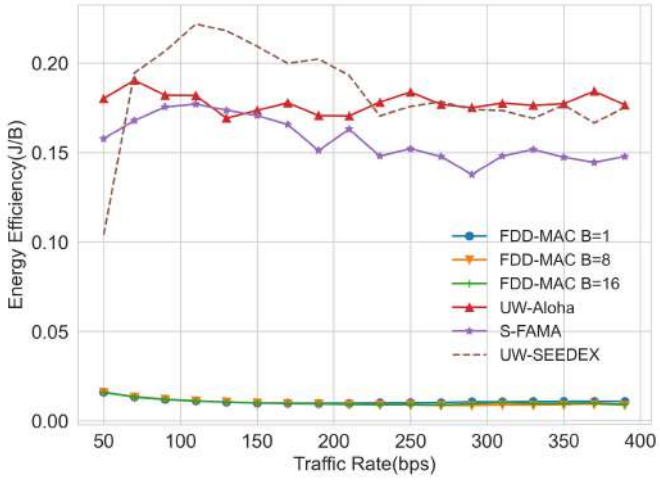

Fig. 24. Energy efficiency of the mesh networks using the four MAC protocols.

evaluation over a broader data rate scale is not provided here because the performance is relatively stable.

VII. Conclusion

In this paper, we analyzed the vector hydrophone and multimodal transducer models and proposed a full-duplex directional MAC framework based on these models, along with a theoretical energy model for the proposed framework. Moreover, an FDD-MAC protocol is elaborated as a benchmark that achieves better channel utilization, end-to-end delay, and energy efficiency compared to the classical MAC protocols designed for UASNs. The results supporting these conclusions were obtained through extensive simulations implemented in NS-3. In the future, we will further improve FDD-MAC and explore additional MAC protocols based on the proposed framework.

References

[1] S. Shahabudeen, M. Motani, and M. Chitre, "Analysis of a high-performance MAC protocol for underwater acoustic networks," *IEEE J. Ocean. Eng.*, vol. 39, no. 1, pp. 74–89, Jan. 2014.

[2] G. Liang, Z. Shi, L. Qiu, S. Sun, and T. Lan, "Sparse Bayesian learning based direction-of-arrival estimation under spatially colored noise using acoustic hydrophone arrays," *J. Mar. Sci. Eng.*, vol. 9, no. 2, p. 127, Jan. 2021.

[3] J. Heidemann, M. Stojanovic, and M. Zorzi, "Underwater sensor networks: Applications, advances and challenges," *Philos. Trans. Roy. Soc. A, Math., Phys. Eng. Sci.*, vol. 370, no. 1958, p. 158, 2012.

[4] P. Casari and M. Zorzi, "Protocol design issues in underwater acoustic networks," *Comput. Commun.*, vol. 34, no. 17, pp. 2013–2025, 2011.

[5] K. Chen, M. Ma, E. Cheng, F. Yuan, and W. Su, "A survey on MAC protocols for underwater wireless sensor networks," *IEEE Commun. Surveys Tuts.*, vol. 16, no. 3, pp. 1433–1447, 3rd Quart., 2014.

[6] E. Gallimore, J. Partan, I. Vaughn, S. Singh, J. Shusta, and L. Freitag, "The WHOI micromodem-2: A scalable system for acoustic communications and networking," in *Proc. OCEANS*, Sep. 2010, pp. 1–7.

[7] WHOI. (2021). *WHOI Micro-Modem*. [Online]. Available: https://acomms.whoi.edu/micro-modem/

[8] M. Stojanovic and J. Preisig, "Underwater acoustic communication channels: Propagation models and statistical characterization," *IEEE Commun. Mag.*, vol. 47, no. 1, pp. 84–89, Jan. 2009.

[9] M. K. Park and V. Rodoplu, "UWAN-MAC: An energy-efficient MAC protocol for underwater acoustic wireless sensor networks," *IEEE J. Ocean. Eng.*, vol. 32, no. 3, pp. 710–720, Jul. 2007.

[10] B. Peleato and M. Stojanovic, "Distance aware collision avoidance protocol for ad-hoc underwater acoustic sensor networks," *IEEE Commun. Lett.*, vol. 11, no. 12, pp. 1025–1027, Dec. 2007.

[11] M. Molins and M. Stojanovic, "Slotted FAMA: A MAC protocol for underwater acoustic networks," in *Proc. OCEANS*, May 2006, pp. 1–7.

[12] A. A. Syed, W. Ye, and J. Heidemann, "T-Lohi: A new class of MAC protocols for underwater acoustic sensor networks," in *Proc. Conf. Comput. Commun. (IEEE INFOCOM)*, Apr. 2008, pp. 231–235.

[13] L. Emokpae and M. Younis, "Reflection-enabled directional MAC protocol for underwater sensor networks," in *Proc. Wireless Days*, Oct. 2011, pp. 1–6.

[14] G. Jakllari, W. Luo, and S. V. Krishnamurthy, "An integrated neighbor discovery and MAC protocol for ad hoc networks using directional antennas," *IEEE Trans. Wireless Commun.*, vol. 6, no. 3, pp. 1024–1114, Mar. 2007.

[15] R. R. Choudhury, X. Yang, N. H. Vaidya, and R. Ramanathan, "Using directional antennas for medium access control in ad hoc networks," in *Proc. 8th Annu. Int. Conf. Mobile Comput. Netw.*, 2002, pp. 59–70.

[16] Q. Gang, S. Gan, S. Liu, L. Ma, and Z. Sun, "Digital self-interference cancellation for asynchronous in-band full-duplex underwater acoustic communication," *Sensors*, vol. 18, no. 6, p. 1700, 2018.

[17] P. Xie and J.-H. Cui, "Exploring random access and handshaking techniques in large-scale underwater wireless acoustic sensor networks," in *Proc. MTS/IEEE OCEANS*, Sep. 2006, pp. 1–6.

[18] R. Petroccia, C. Petrioli, and J. Potter, "Performance evaluation of underwater medium access control protocols: At-sea experiments," *IEEE J. Ocean. Eng.*, vol. 43, no. 2, pp. 547–556, Apr. 2018.

[19] C. Petrioli, R. Petroccia, and M. Stojanovic, "A comparative performance evaluation of MAC protocols for underwater sensor networks," in *Proc. OCEANS*, Sep. 2008, pp. 1–10.

[20] L. T. Tracy and S. Roy, "A reservation MAC protocol for ad-hoc underwater acoustic sensor networks," in *Proc. WuWNeT*, 2014, pp. 95–98.

[21] J. Zhang, X. Ma, G. Qiao, and C. Wang, "A full-duplex based protocol for underwater acoustic communication networks," in *Proc. OCEANS, San Diego*, 2014, pp. 1–6.

[22] C. Li *et al.*, "FDCA: A full-duplex collision avoidance MAC protocol for underwater acoustic networks," *IEEE Sensors J.*, vol. 16, no. 11, pp. 4638–4647, Jun. 2016.

[23] X. Zhuo, M. Liu, F. Qu, Y. Wei, and J. Li, "A two-fold handshaking full-duplex MAC protocol for underwater acoustic communication networks," in *Proc. Int. Conf. Underwater Netw. Syst. (WuWNeT)*. New York, NY, USA: Association for Computing Machinery, Oct. 2019, pp. 1–2.

[24] A. Abdullah, L. Cai, and F. Gebali, "DSDMAC: Dual sensing directional MAC protocol for ad hoc networks with directional antennas," *IEEE Trans. Veh. Technol.*, vol. 61, no. 3, pp. 1266–1275, Mar. 2012.

[25] W. Na, L. Park, and S. Cho, "Deafness-aware MAC protocol for directional antennas in wireless ad hoc networks," *Ad Hoc Netw.*, vol. 24, pp. 121–134, Jan. 2015.

[26] H. Gossain, C. Cordeiro, T. Joshi, and D. P. Agrawal, "Cross-layer directional antenna MAC protocol for wireless *ad hoc* networks," *Wireless Commun. Mobile Comput.*, vol. 6, no. 2, pp. 171–182, 2010.

[27] H. Li and Z. Xu, "Self-adaptive neighbor discovery in mobile ad hoc networks with directional antennas," in *Proc. IEEE Int. Conf. Commun. Workshops (ICC Workshops)*, May 2018, pp. 1–6.

[28] Z. H. Mir, W.-S. Jung, and Y.-B. Ko, "Continuous neighbor discovery protocol in wireless ad hoc networks with sectored-antennas," in *Proc. IEEE 29th Int. Conf. Adv. Inf. Netw. Appl.*, Mar. 2015, pp. 54–61.

[29] L. Chen, Y. Li, and A. V. Vasilakos, "On oblivious neighbor discovery in distributed wireless networks with directional antennas: Theoretical foundation and algorithm design," *IEEE/ACM Trans. Netw.*, vol. 25, no. 4, pp. 1982–1993, Aug. 2017.

[30] B. El Khamlichi, D. H. N. Nguyen, J. E. Abbadi, N. W. Rowe, and S. Kumar, "Collision-aware neighbor discovery with directional antennas," in *Proc. Int. Conf. Comput., Netw. Commun. (ICNC)*, Mar. 2018, pp. 220–225.

[31] F. N. Nur *et al.*, "Collaborative neighbor discovery in directional wireless sensor networks: Algorithm and analysis," *EURASIP J. Wireless Commun. Netw.*, vol. 2017, no. 1, p. 119, Dec. 2017.

[32] J. L. Butler, A. L. Butler, and J. A. Rice, "A tri-modal directional transducer," *J. Acoust. Soc. Amer.*, vol. 115, no. 2, pp. 658–665, Feb. 2004.

[33] Y. Zhang, D. Sun, and D. Zhang, "Robust adaptive acoustic vector sensor beamforming using automated diagonal loading," *Appl. Acoust.*, vol. 70, no. 8, pp. 1029–1033, Aug. 2009.

[34] H. Junying, *Fundamentals of Vector Acoustic Signal Processing*. Beijing, China: National Defense Industry Press, 2009.

[35] B. Abraham, "Ambient noise measurements with vector acoustic hydrophones," in *Proc. OCEANS*, Sep. 2006, pp. 1–7.
[36] J. L. Butler, A. L. Butler, and S. C. Butler, "The modal projector," *J. Acoust. Soc. Amer.*, vol. 129, no. 4, pp. 1881–1889, Apr. 2011.
[37] B. Liu and J. Lei, *Principles of Underwater Sound*. Harbin, China: Harbin Engineering University Press, 2010.
[38] R. F. Coates, *Underwater Acoustic Systems*. New York, NY, USA: Macmillan, 1990.
[39] Z. Chen, "Volume and area of revolution under polar coordinate system," *Stud. College Math.*, vol. 15, no. 6, pp. 9–11, 2012.
[40] J. Zhang, X. Xu, Z. Chen, M. Bao, X.-P. Zhang, and J. Yang, "High-resolution DOA estimation algorithm for a single acoustic vector sensor at low SNR," *IEEE Trans. Signal Process.*, vol. 68, pp. 6142–6158, 2020.
[41] J. Hui, H. Liu, Y. U. Huabing, and M. Fan, "Study on the physical basis of pressure and particle velocity combined processing," *Acta Acustica*, vol. 4, pp. 303–307, Apr. 2000.
[42] T. Nitsche, C. Cordeiro, A. B. Flores, E. W. Knightly, E. Perahia, and J. C. Widmer, "IEEE 802.11ad: Directional 60 GHz communication for multi-gigabit-per-second Wi-Fi [invited paper]," *IEEE Commun. Mag.*, vol. 52, no. 12, pp. 132–141, Dec. 2014.
[43] A. Akhtar and S. C. Ergen, "Directional MAC protocol for IEEE 802.11ad based wireless local area networks," *Ad Hoc Netw.*, vol. 69, pp. 49–64, Feb. 2018.
[44] R. R. Choudhury and N. H. Vaidya, "Deafness: A MAC problem in ad hoc networks when using directional antennas," in *Proc. IEEE Int. Conf. Netw. Protocols*, Oct. 2004, pp. 283–292.
[45] H. U. Yildiz, V. C. Gungor, and B. Tavli, "Packet size optimization for lifetime maximization in underwater acoustic sensor networks," *IEEE Trans. Ind. Informat.*, vol. 15, no. 2, pp. 719–729, Feb. 2018.
[46] Z. Peng, Z. Zhou, J.-H. Cui, and Z. J. Shi, "Aqua-Net: An underwater sensor network architecture: Design, implementation, and initial testing," in *Proc. OCEANS*, Oct. 2009, pp. 1–8.
[47] E. Camarajunior, L. Vieira, and M. Vieira, "UW-SEEDEX: A pseudorandom-based MAC protocol for underwater acoustic networks," *IEEE Trans. Mobile Comput.*, early access, Jan. 18, 2021. [Online]. Available: https://ieeexplore.ieee.org/document/9328336, doi: 10.1109/TMC.2021.3052754.
[48] (2021). *NS-3*. [Online]. Available: https://www.nsnam.org/
[49] M. Stojanovic, "On the relationship between capacity and distance in an underwater acoustic communication channel," *ACM SIGMOBILE Mobile Comput. Commun. Rev.*, vol. 11, no. 4, pp. 34–43, 2007.

Qipei Liu received the B.S. degree in electronic and information engineering from the College of Information Engineering, North China University of Water Resources and Electric Power, Zhengzhou, China, in 2012. He is pursuing the Ph.D. degree in information and communication engineering with the College of Underwater Acoustic Engineering, Harbin Engineering University, Harbin, China.

His research interests include architecture and protocol design of underwater acoustic sensor networks, ad-hoc networks, algorithms, and artificial intelligence.

Gang Qiao received the B.S., M.S., and Ph.D. degrees from the College of Underwater Acoustic Engineering, Harbin Engineering University (HEU), China, in 1996, 1999, and 2004, respectively.

Since 1999, he has been working at HEU, where he is presently a Professor and the Dean of the College of Underwater Acoustic Engineering, HEU. He has already published more than 80 papers and owned seven national invention patents. His current research interests include underwater communication and networks, detection and positioning of underwater targets, and sonar designed for small carriers. He is a member of the Acoustical Society of China and the Youth Federation of Heilongjiang Province and the Vice Chairperson of the Robotics Society of Heilongjiang Province. He won the National Award for the outstanding scientific and technological workers and the Science and Technology Award for young talents in Heilongjiang province.

Suleman Mazhar (Senior Member, IEEE) received the Ph.D. degree from Tokyo University, Japan.

He completed his Postdoctoral Research at Georgetown University, Washington, DC, USA. He is currently a Professor with the College of Underwater Acoustic Engineering, Harbin Engineering University, China. He loves teaching machine learning and data science and spends leisure time in field work, protecting endangered species in the rivers and endangered beings on the roads. His research interests include acoustics and machine learning.

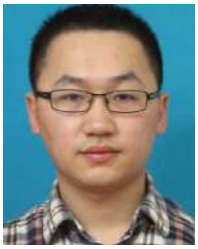

Songzuo Liu (Member, IEEE) received the B.S. and Ph.D. degrees in signal and information processing from the College of Underwater Acoustic Engineering, Harbin Engineering University (HEU), China, in 2008 and 2014, respectively.

From 2015 and 2017, he was a Postdoctoral Researcher with the Underwater Wireless Sensor Networking (UWSN) Group, SENSE Laboratory, Sapienza University of Rome. He is currently an Associate Professor with the College of Underwater Acoustic Engineering, Harbin Engineering University. His research interests include covert underwater acoustic communication and passive acoustic monitoring of cetaceans.

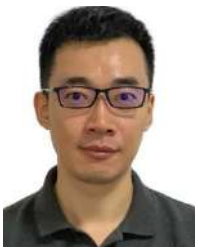

Yi Lou (Member, IEEE) received the B.S. degree in communication engineering from Jilin University, Jilin, China, in 2009, and the M.S. and Ph.D. degrees in information and communication engineering from the Harbin Institute of Technology, Harbin, China, in 2013 and 2017, respectively.

He was a Visiting Student at The University of British Columbia, Kelowna, BC, Canada, in 2016. He is currently an Associate Professor with the College of Underwater Acoustic Engineering, Harbin Engineering University, Harbin. His research interests include cooperative communications, underwater wireless optical communication, and underwater acoustic communication.